International Journal of Engineering & Technology, 5 (2) (2016) 51-57

International Journal of Engineering & Technology

Website: www.sciencepubco.com/index.php/IJET
doi: 10.14419/ijet.v5i2.6113
Research paper

Welding cooling rate effects on microstructure of an API 5l x100 steel

Diego Aires De Freitas [1]*, Ivan Guerra Machado [1], José Antônio Esmério Mazzaferro [2], Arnaldo Ruben Gonzalez [2], Cintia Cristiane Petry Mazzaferro [2]

[1] Federal University of Rio Grande do Sul, PPGE3M, Welding & Related Techniques Laboratory
[2] Federal University of Rio Grande do Sul, PROMEC, Welding & Related Techniques Laboratory Porto Alegre, RS, Brazil
**Corresponding author E-mail: diego_freitas@ymail.com*

Abstract

The aim of this work was to investigate the influence of five different cooling rates on properties of weld metal (WM) and heat affected zone (HAZ) of an API 5L X100 steel welded by GMAW. Bead on pipe (BOP) welds were made on 100x300 mm sections of a 15.8 mm thickness and 580 mm outside diameter API 5L X100 pipe, through five preheat temperatures (-30, 34, 100, 150 and 200 °C), aiming to obtain different cooling rates. Thermocouples were used to obtain the cooling time from 800 to 500 ºC ($\Delta t_{8/5}$) during welding. The microstructures of base metal (BM) and HAZ were analyzed by light microscopy and scanning electron microscopy (SEM). Hardness measurements were made on the BOP welds in order to identify maximum and minimum values. As expected, due to the different cooling rates during welding, the distinct preheat temperatures have influenced the weld properties. Maximum and minimum HAZ microhardness, and weld metal hardness decrease as the preheat temperature increases. HAZ area, grain size of fine grained HAZ and coarse grained HAZ increase with increasing preheat temperature.

Keywords: *Welding; API 5l X100 Steel; Cooling Rate; Mechanical Properties; Heat Affected Zone.*

1. Introduction

API 5L X100 is a high strength low alloy steel (HSLA) used in pipelines for transportation of oil and gas. High strength in X100 steel is reached by a controlled manufacturing process that aims a steel with a microstructure containing bainite and martensite.
Higher strength steels enable the use of thinner walled pipe (less than 10 mm) at greater operating pressures [1]. Thinner walled pipes enable costs reductions by material saving. This also resulted in a reduction of the pipelaying costs, because of reduced pipe transportation costs and greatly reduced welding costs, through reduced welding times needed with thinner walls [2]. Using an X100 steel high pressure pipes could give investment costs savings of about 7% with respect to X80 grades. When X70 and X100 are compared, cost savings of up to 30% are possible [3].
The use of X100 steel for pipelines is relatively recent and there is still some need for studies about the welding of this material. Information about maximum and minimum HAZ hardness, weld metal hardness, HAZ area and weld microstructure are essential to use X100 for pipelines. For this reason, welds with different cooling rates were performed in this work.
This work aims to investigate the cooling rate effects on microstructure and mechanical properties of an API 5L X100 steel, by analyzing heat affect zone, base metal and weld metal properties.

2. Experimental

2.1. Welding procedure

Bead on pipe (BOP) welds were made with MAG process through a robot and synergic power source. The shielding gas used was a mixture of 90% Ar and 10% CO_2, with a flow rate of 15 L/min. ER120S-G wire (1.2 mm gauge) was used as filler metal. The following conditions were employed for the bead on pipe welds: wire speed rate of 6.5 m/min; voltage of 22.4 V; weld speed of 8.0 mm/s, and contact tip to work distance of 20 mm. The heat input of about 0.69 kJ/mm was the same for all weldments. These welding conditions were chosen because they presented suitable deposition rate and weld penetration to be used for the multi-pass weld of this pipe section.
The welds were made on 100x300 mm sections of a 15.8 mm thickness and 580 mm outside diameter API 5L X100 pipe. Five preheat temperatures (-30, 34, 100, 150 and 200 °C) were used aiming to obtain different cooling rates in weld metal (WM) and heat affected zone (HAZ) during welding. The pipe section welded at -30 °C was cooled with liquid nitrogen. The nitrogen was continuously added on the pipe section until it could be noticed that temperature was stable at -30 °C before the weld starts (information provided by thermocouples). The pipe section welded at 34 °C was made at room temperature and the ones made at 100, 150 and 200 °C were heated with a heating torch.
Thermocouples type S were used to obtain $\Delta t_{8/5}$ values (cooling time from 800 to 500ºC) in weld metal and thermocouples type K were used to control the preheat temperature.
To obtain weld metal chemical composition, five layers with five weld passes were deposited on a low carbon steel plate section (using the same conditions employed on BOP welds). After welding, the specimen surface was machined, prepared and analyzed by an optical emission spectrometer. Table 1 presents the chemical composition of the weld metal deposition without dilution.

Table 1: Weld Metal Chemical Composition (Weight %)

Weld Metal Chemical Composition (mass %)					
C	Si	Mn	P	S	Cr
0.0746	0.5130	1.4100	0.0080	0.0088	0.2630
Al	Ni	Cu	Mo	Co	Ti
0.0027	1.5000	0.0175	0.4300	<0.0100	0.0011
V	Nb	Sn	W	Pb	B
<0.0010	<0.0010	0.0012	<0.0100	<0.0020	0.0002

2.2. Microstructure characterization

The welds microstructures were analyzed by light microscopy and scanning electron microscopy (SEM). The specimens were submitted on standard metallography procedures, such as cutting, wet sanding and polishing. For revealing the BOP welds microstructures, a chemical etching using Nital 4% was performed for light microscopy and Nital 2% for SEM. Weld microstructures images were made using a light microscope connected to a digital camera. SEM and light microscope images were taken approximately 1 mm below the sample surface with the purpose to correlate microstructure with hardness tests results performed at the same region.
The BOP welds regions, such as base metal (BM), weld metal (WM) and HAZ, can be easily seen on macrographs. The HAZ regions were classified as follow: Subcritical HAZ (SCHAZ); Intercritical HAZ (ICHAZ); Fine Grained HAZ (FGHAZ) and Coarse Grained HAZ (CGHAZ) [4]. SCHAZ cannot be seen with light microscopy. The other regions can be easily seen by stereo and light microscope due their different coloration and microstructures.
The macrographs were acquired using a stereo microscope due its low magnification. These images were made for measuring HAZ area, melted base metal area and dilution with ImageJ software. As SCHAZ cannot be seen by light microscope, total HAZ area used on the graphs includes only CGHAZ, FGHAZ and ICHAZ.

2.3. Base metal

API 5L X100 steel was employed as base metal in this work. Table 2 presents the chemical composition of the steel used in this work.

Table 2: Chemical Composition of the API 5L X100 Steel (Weight %)

Base Metal Chemical Composition (mass %)					
C	Si	Mn	P	S	Cr
0.0632	0.2960	2.0200	0.0053	<0.0010	0.3670
Al	Ni	Cu	Mo	Co	Ti
0.0295	0.0200	0.0135	0.2000	<0.0100	0.0125
V	Nb	Sn	W	Pb	B
<0.0010	0.0392	<0.0010	<0.0100	<0.0020	<0.0001

Equation (1) was chosen to determine the carbon equivalent (CE). CE_{Pcm} is used for steels with carbon content below 0.12% [5]. The calculated CE_{Pcm} value for the base metal steel used is 0.2068. Using weld metal (without dilution) chemical composition from Table 1, the weld metal CE_{Pcm} value of 0.2309 was calculated. Weld metal CE_{Pcm} is about 18% greater than base metal CE_{Pcm}. Mechanical properties of the steel used were previously evaluated by tensile tests. The values of yield stress of 695 MPa, tensile strength of 751 MPa and elongation of 23.3% were obtained.

$$CE_{Pcm} = C + \frac{Si}{30} + \frac{Mn}{20} + \frac{Cu}{20} + \frac{Ni}{60} + \frac{Cr}{20} + \frac{Mo}{15} + \frac{V}{10} + 5B \quad (1)$$

2.4. Hardness tests

Hardness measurements were made on the bead on pipe welds in order to identify maximum and minimum values. Vickers hardness 5 kg (HV5) values were measured with a hardness tester, with a 5 kg load for 10 s. The measurements were performed on the different regions of the weld (BM, HAZ and WM). The HV5 measurements were made approximately 1 mm below the sample surface, passing through BM, HAZ and WM.

Microhardness tests were performed by a Vickers hardness tester for investigating maximum and minimum values on HAZ and WM. In order to plot graphs with minimum and maximum microhardness as functions of HAZ, SCHAZ microhardness were not included because its measurements were not made in this area. However, a graph with SCHAZ microhardness as function of preheat temperature and $\Delta t_{8/5}$ was also presented in this work. A load of 0.2 kg was applied for 15 seconds and 0.25 mm of spacing between each measurement. This load value was chosen in order to identify the maximum and minimum microhardness values analyzing a small limited area of each HAZ region. As shown in Fig. 1, the measurements were made following a bottom line, a left line and a right line (1.0 mm bellow the sample surface), from BM to WM-HAZ interface.

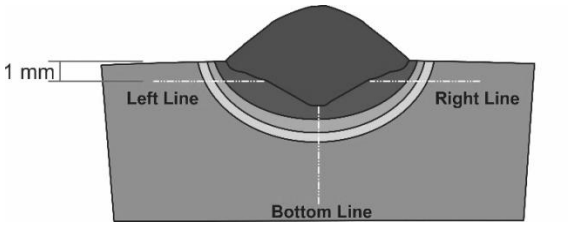

Fig. 1: Microhardness Measurements Locations on BOP Welds.

3. Results and discussion

3.1. Welds cooling rates

Fig. 2 shows weld metal cooling time from 800 to 500°C ($\Delta t_{8/5}$) measured as function of preheat temperature. It can be seen that $\Delta t_{8/5}$ and preheat temperature almost exhibit linear behavior between each other.

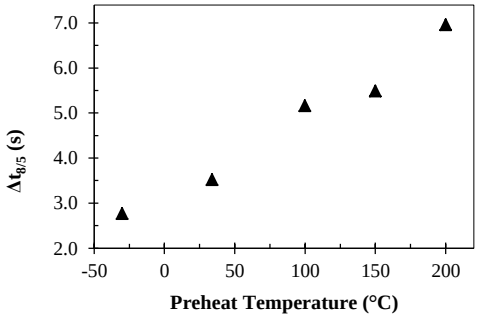

Fig. 2: Weld Metal $\Delta t_{8/5}$ Values Measured for Different Preheat Temperatures.

This almost linear behavior relationship between $\Delta t_{8/5}$ and preheat temperature is described by Equation (2), where H is the heat input, T_0 is the preheat temperature and k is the thermal conductivity of the material [6].

$$\Delta t_{8/5} = \frac{H}{2\pi k}\left(\frac{1}{500-T_0}\right) - \left(\frac{1}{800-T_0}\right) \quad (2)$$

3.2. Light microscopy

3.2.1. Macrographs

Fig. 3 presents a macrograph for the weld made at 150 °C. Base metal, weld metal, coarse grained HAZ (CGHAZ), fine grained HAZ (FGHAZ) and intercritical HAZ (ICHAZ) could be easily identified in this macrograph. SCHAZ is located in a small arc-shaped region between ICHAZ and base metal and could not be seen in this macrograph.

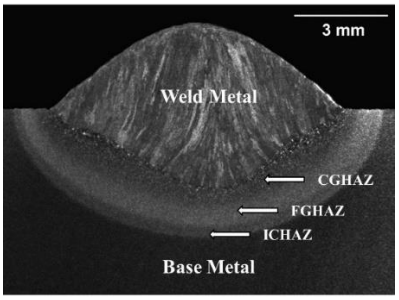

Fig. 3: Weld Metal, HAZ Regions and Base Metal in the Bead on Pipe Weld Made at 150 °C.

Fig. 4 and Fig. 5 shows the areas of HAZ and melted base metal as functions of preheat temperature and $\Delta t_{8/5}$, with average, upper and lower limits represented on the graph.

In Fig. 4, it can be noticed that with a preheat temperatures increment, HAZ area tends to increase. The higher the preheat temperature, the greater the HAZ area due to lower cooling rates associated to greater preheat temperatures.

Analyzing Fig. 5, it can be observed that melted base metal area has increased from -30 to 100 °C. However, it had its value decreased about 1% when 150 °C were used as preheat temperature. From preheat temperature of 150 to 200 °C, melted base metal area has increased approximately 5%. This behavior were completely different from HAZ area when preheat temperature increased. It could be explained by a higher standard deviation in the measurements of the melted base metal area.

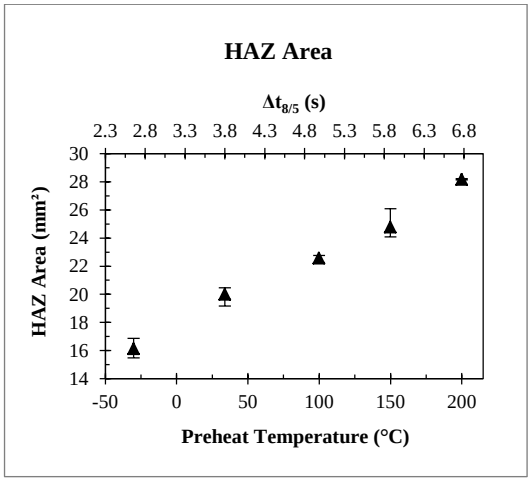

Fig. 4: HAZ Area as Function of Preheat Temperatures and $\Delta t_{8/5}$.

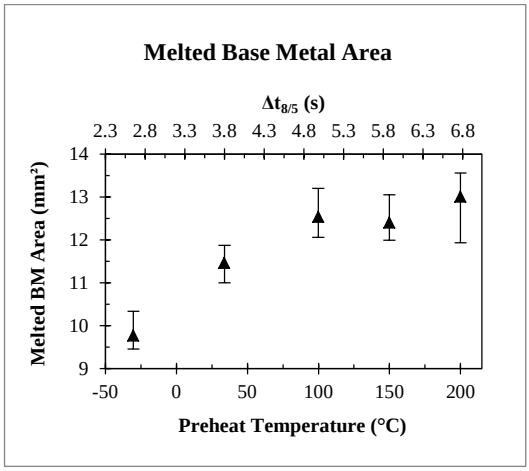

Fig. 5: Melted Base Metal Area as Function of Preheat Temperatures and $\Delta t_{8/5}$.

Fig. 6 shows the measured dilution as function of preheat temperatures and $\Delta t_{8/5}$. Maximum dilution value of 45% occurs at 200 °C. Dilution increases with temperature due a higher weld penetration and higher melted base metal area as the temperature increases.

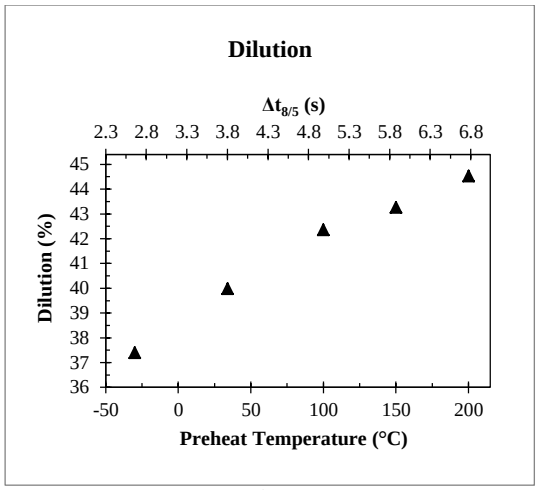

Fig. 6: Dilution as Function of Preheat Temperatures and $\Delta t_{8/5}$.

Using base metal CE_{Pcm} (0.2068), pure weld metal CE_{Pcm} (0.2309) and dilution values, the CE_{Pcm} values for weld metals were calculated (Table 3). Analyzing data from Table 3, it can be notice that there are small differences between weld metals CE_{Pcm} welded at different temperatures. The biggest CE_{Pcm} value (BOP weld made at -30 °C) is only 0.77% greater than the smallest one (BOP weld made at 200 °C).

Table 3: Calculated Weld Metal Ce_{pcm} Values for Different Preheat Temperatures.

Temperature (°C)	-30	34	100	150	200
CE_{Pcm} (Weight %)	0.2219	0.2212	0.2207	0.2205	0.2201

3.2.2. Micrograph

Fig. 7 and Fig. 8 show the microstructures for the fine grained HAZ and coarse grained HAZ for the weld made at 34 °C.

Fig. 9 and Fig. 10 shows the microstructures for the fine grained HAZ and coarse grained HAZ for the weld made at 150 °C. Comparing Fig. 7 and Fig. 8 with Fig. 9 and Fig. 10, it can be noticed that in both cases the weld made at 150 °C presented higher grain size due a lower cooling rate for this preheat temperature. On CGHAZ, martensite and bainite can be observed.

Phase identification could not be done in base metal and subcritical HAZ with this magnification. For this reason, SEM analysis were performed.

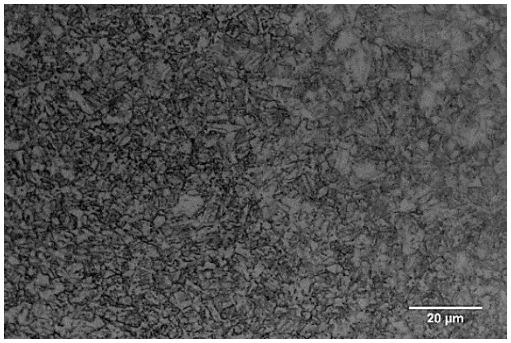

Fig. 7: Fine Grained HAZ for the Weld Made at 34 °C.

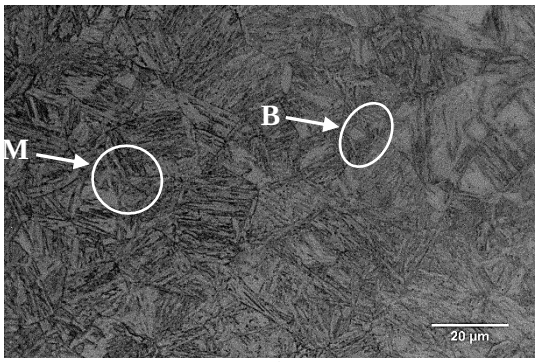

Fig. 8: Coarse Grained HAZ for the Weld Made at 34 °C.

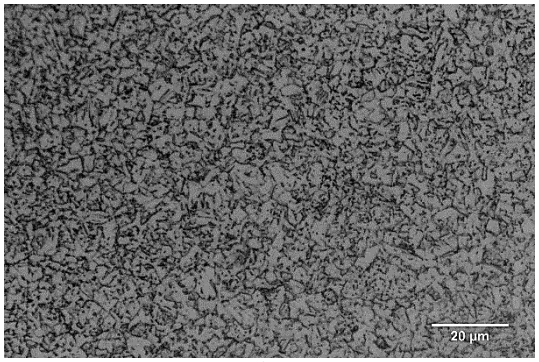

Fig. 9: Fine Grained HAZ for the Weld Made at 150 °C.

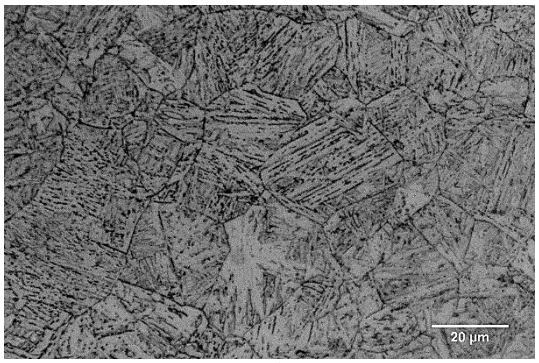

Fig. 10: Coarse Grained HAZ for the Weld Made at 150 °C.

3.3. SEM

Fig. 11 shows de base metal microstructure. The base metal microstructure is composed by martensite islands, bainite and retained austenite (white spots).

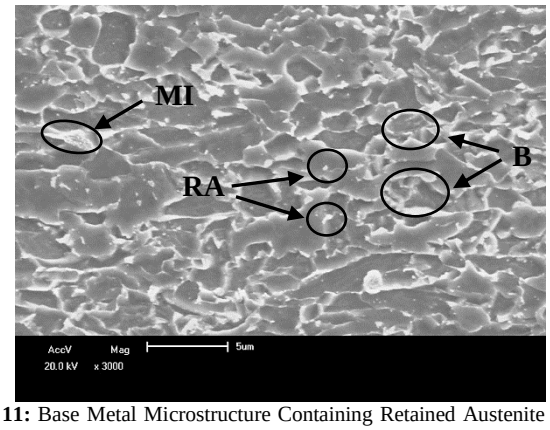

Fig. 11: Base Metal Microstructure Containing Retained Austenite (RA), Martensite Islands (MI) and Bainite (B).

Fig. 12 shows the subcritical HAZ for the weld made at 34 °C. Comparing base metal microstructure (Fig. 11) with subcritical HAZ microstructure, a difference of morphology can be noticed, due to partial spheroidisation of carbides. Fig. 13 shows the Intercritical HAZ for the weld made at 34 °C. Islands of martensite, retained austenite and bainite can be observed.

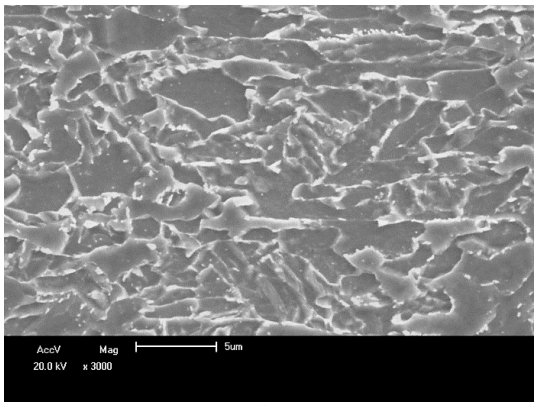

Fig. 12: Subcritical HAZ for the Weld Made at 34 °C.

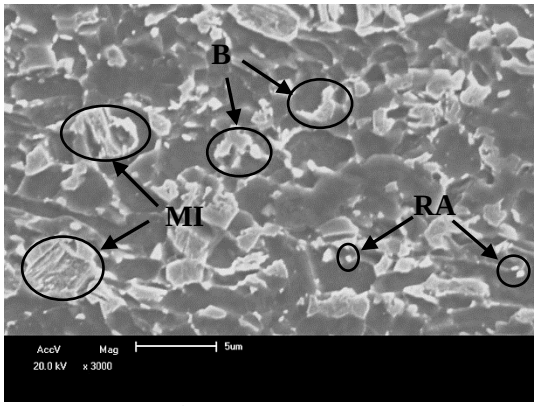

Fig. 13: Intercritical HAZ for the Weld Made at 34 °C. Retained Austenite (RA), Martensite Islands (MI) and Bainite (B) Can Be Observed.

Fig. 14 shows the fine grained HAZ for the weld made at 34 °C. The grain size is smaller, if compared with the other HAZ regions. Due to the smaller grain size associated to small martensite islands dispersed on the parent metal, this region presents higher hardness values than intercritical and subcritical HAZ.

Fig. 15 presents the coarse grained HAZ for the weld made at 34 °C. Grain size increases due to the higher temperatures near the weld metal. Martensite and coalesced bainite (CB) can be seen in this HAZ region. This region presented the highest hardness values due the presence of more phases with high hardness than other regions.

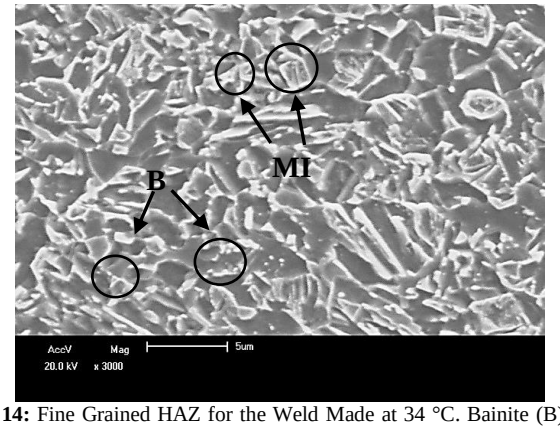

Fig. 14: Fine Grained HAZ for the Weld Made at 34 °C. Bainite (B) and Martensite Islands (MI) Can Be Observed.

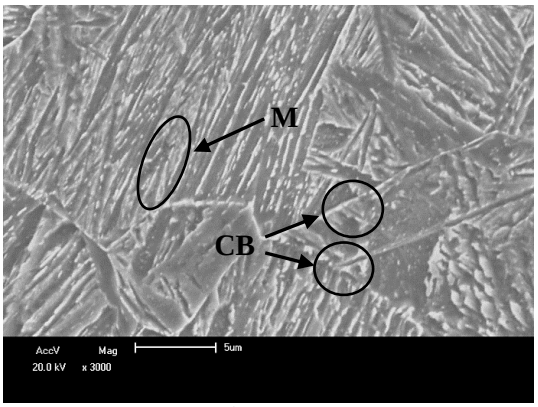

Fig. 15: Coarse Grained HAZ for the Weld Made at 34 °C. Coalesced Bainite (CB) and Martensite (M) Can Be Observed.

Fig. 16 and Fig. 17 show the SEM images for the fine grained HAZ and coarse grained HAZ for the weld with 200 °C as preheat temperature.

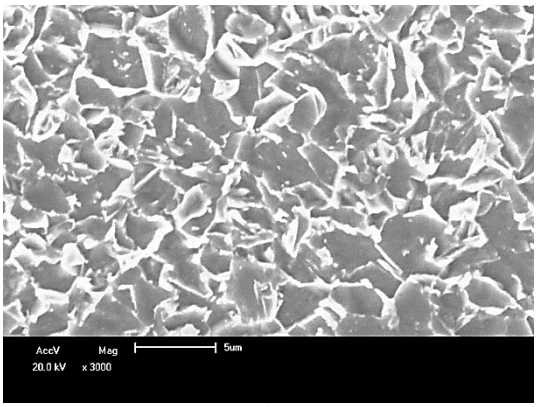

Fig. 16: Fine Grained HAZ for the Weld Made at 200 °C.

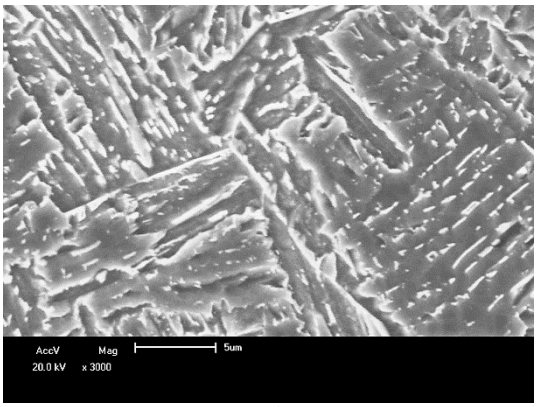

Fig. 17: Coarse Grained HAZ for the Weld Made at 200 °C.

Comparing Fig. 14 and Fig. 15 with Fig. 16 and Fig. 17, it can be noticed that the weld made at 200 °C presented greater grain size for both coarse grained and fine grained HAZ. It can explained because greater preheat temperatures generates greater grain sizes due to slower cooling rates associated to higher temperatures.

3.4. Hardness tests

3.4.1. Vickers hardness

Fig. 18 provides the average weld metal hardness (HV5) as function of temperature. A linear behavior between temperature and weld metal hardness can be noticed. As discussed previously on section 3.2.1, CE_{Pcm} are practically the same for weld metals, with a difference of only 0.0017% between the largest and the smallest value of CE_{Pcm}. Knowing this information, it is possible to say that weld metal hardness values were mostly influenced by cooling rate during welding. In addition, average weld metal hardness decreases as the preheat temperature and $\Delta t_{8/5}$ increase.

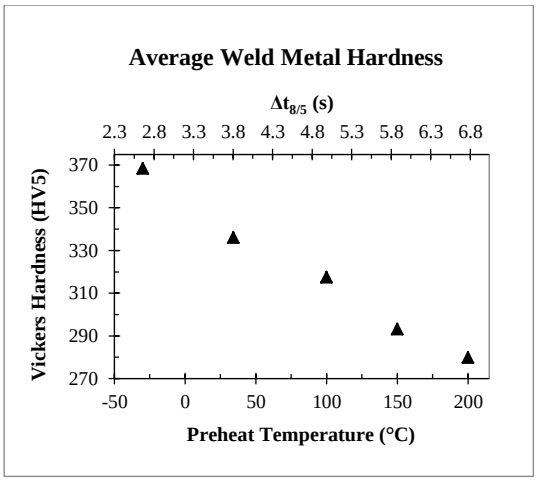

Fig. 18: Average Weld Metal Hardness as Function of Preheat Temperature and $\Delta t_{8/5}$.

On the other hand, Fig. 19 presents the results obtained on hardness tests (HV5) measured through the weld cross section. From BM to SCHAZ, the microhardness decreases due to a difference of morphology caused by partial spheroidisation of carbides. ICHAZ presented similar hardness values if compared with minimum SCHAZ hardness. From SCHAZ to FGHAZ the hardness increases due to a greater martensite island formation. CGHAZ presented an increment in hardness due to martensite formation.

It can be noticed that all BOP welds had their hardness decreased at base metal region before HAZ beginning. HAZ and weld metal hardness presented lowers values for welds with greater preheat temperatures.

Intercritical HAZ presented the minimum hardness values and coarse grained HAZ presented higher hardness values on HAZ. Comparing Vickers hardness (HV5) of the welds made at different temperatures, it can be noticed that HAZ hardness decreases as the preheat temperature increases.

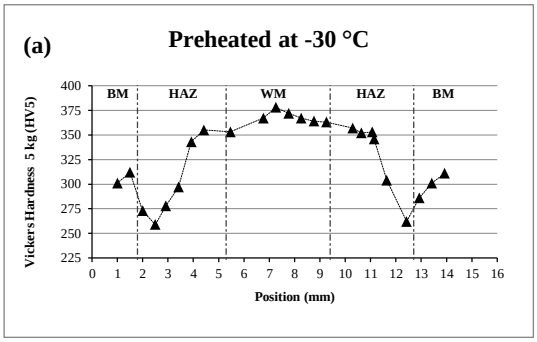

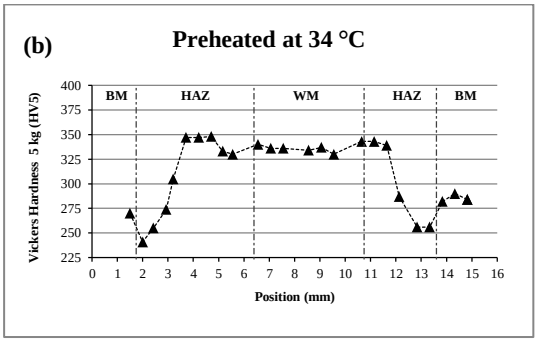

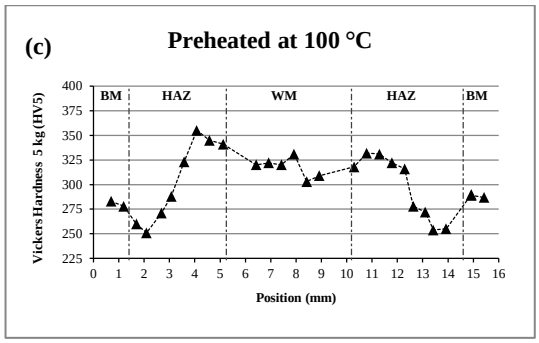

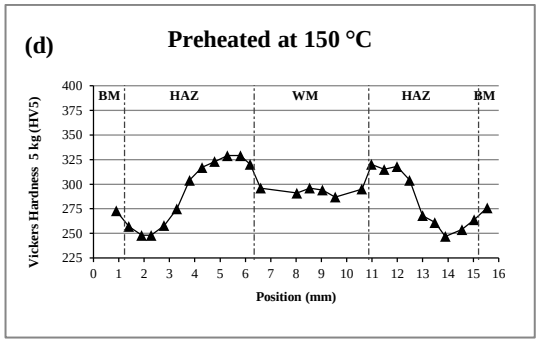

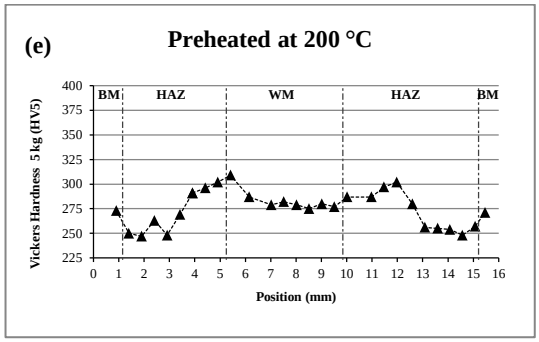

Fig. 19: Measured Values of HV5 for the Bead on Pipe Welds Preheated at (A) -30, (B) 34, (C) 100, (D) 150 and (E) 200 °C.

3.4.2. Vickers microhardness

Fig. 20 shows maximum and minimum HAZ microhardness as functions of preheat temperature and $\Delta t_{8/5}$. Welds made at low temperatures presented greater maximum microhardness due to their higher cooling rates if compared to the ones made at higher temperatures. All the welds presented their maximum values of microhardness in the CGHAZ.

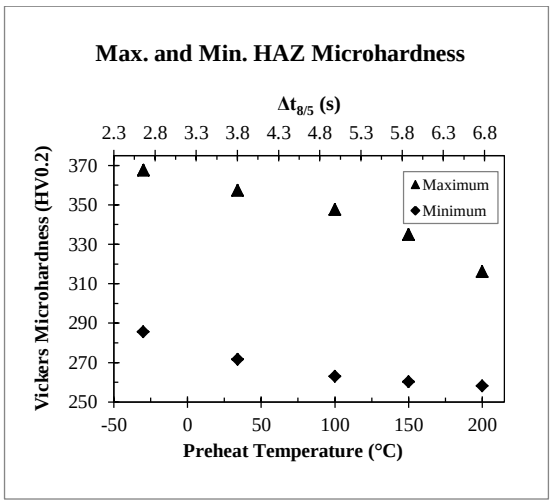

Fig. 20: Maximum and Minimum Vickers Microhardness as Functions of Preheat Temperature and $\Delta t_{8/5}$.

Fig. 21 shows maximum and minimum HAZ microhardness as functions of total HAZ area. Analyzing both graphs, we can affirm that in both cases HAZ maximum and minimum microhardness decrease as the HAZ area increases.

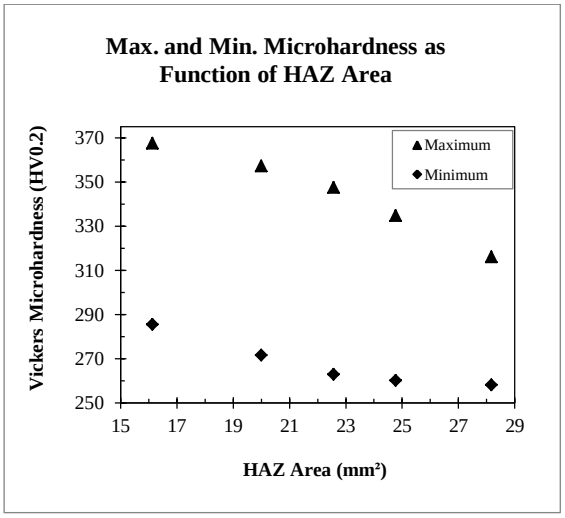

Fig. 21: Maximum and Minimum Vickers Microhardness as Functions of Total HAZ Area.

Fig. 22 presents the minimum microhardness at SCHAZ as function of preheat temperature and $\Delta t_{8/5}$. Minimum microhardness at SCHAZ decreases when the preheat temperature decreases from -30 to 33 °C (decreasing of 9.3 HV0.2). For greater preheat temperatures, from 33 to 200 °C, the minimum microhardness presented slight increases as the preheat temperature increases (variation of 4.1 HV0.2).

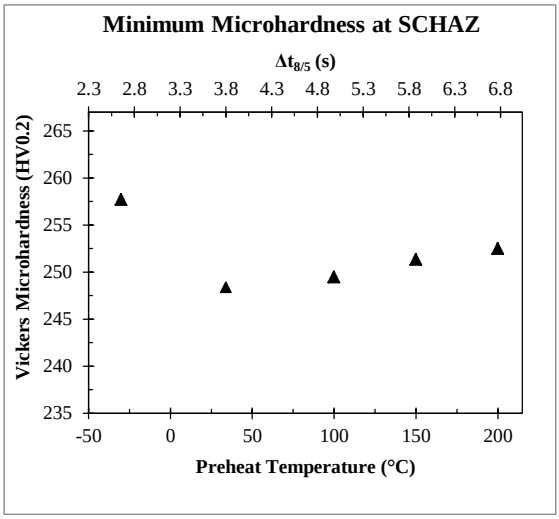

Fig. 22: Minimum Microhardness at Subcritical HAZ As Function of Preheat Temperature And $\Delta t_{8/5}$.

4. Conclusions

Based on the results presented on the previous sections of this work, the following conclusions were made:

- There is almost linear behavior between $\Delta t_{8/5}$ and the preheat temperature for the conditions of this study.
- The grain size of the fine grained HAZ and coarse grained HAZ increases with increasing preheat temperature.
- Phase transformations on HAZ have influenced the mechanical properties of welds.
- The presence of martensite made the hardness increases on CGHAZ.
- Minimum and maximum HAZ microhardness (HV0.2) were influenced by cooling rate during welding. The maximum

and minimum HAZ microhardness decrease as the preheat temperature increases.

- Minimum HAZ microhardness values were found on the intercritical HAZ and maximum HAZ microhardness values were found on the coarse grained HAZ for all weldments.
- Weld metal hardness HV5 decreases with increasing preheat temperature and $\Delta t_{8/5}$ due to lower cooling rates associated to higher preheats temperatures. As the CE_{Pcm} are practically the same for all weld metals, weld metal hardness is mostly influenced by temperature and $\Delta t_{8/5}$.
- HAZ area and dilution increase as the preheat temperature increases.
- Measurements made on macrograph tests shown that HAZ area and dilution increases with increasing temperature.

Acknowledgements

The authors would like to thank to CNPQ (Brazil) for granting the master's scholarship to one of the authors (DAF); to LAMEF, where the hardness Vickers 5 kg (HV5) measurements and chemical analysis were performed; and to ESAB Brasil for the donation of the welding consumable (AristoRod™ 79) used in this study.

References

[1] Thewlis, G., Weldability of X100 Linepipe - *Science and Technology of Welding and Joining*, 2000, VOL5 N° 6. http://dx.doi.org/10.1179/136217100101538434.

[2] M. K. Gräf, H. G. Hillenbrand, C. J. Heckman and K. A. Niederhoff, High-strength large pipe for long-distance high pressure gas pipelines, *Int. J. Offshore Polar Eng.*, 2004, 14, 69–74.

[3] L. Barsanti, H. G. Hillenbrand, Possible use of new materials for high pressure line pipe construction: The experience of SNAM RETE GAS and EUROPIPE on X 100 grade steel, Proceedings of IPC: *The International Pipeline Conference, Calgary*, Alberta, Canada, 2002. http://dx.doi.org/10.1115/IPC2002-27089.

[4] Hudson, M. G., Welding of X100 Linepipe. 2004. PhD Thesis – School of Industrial and Manufacturing Science. Cranfield University.

[5] American Petroleum Institute, *API Specification 5L/ISO 3183*, 2009.

[6] Machado, I. G., *Condução do Calor na Soldagem: Fundamentos & Aplicações.* Porto Alegre, 2000. v. 1. 101p.